



XA04N0702

OUTAGE RISK ASSESSMENT AND MANAGEMENT (ORAM) THERMAL-HYDRAULICS TOOLKIT

V.E. Denny, A.T. Wassel, F. Issacci
Science Applications International Corporation (SAIC)
21151 Western Avenue
Torrance, CA 90501-1724

S. Pal Kalra
Electric Power Research Institute (EPRI)
3412 Hillview Avenue
Palo Alto, CA 94303

ABSTRACT

A PC-based thermal-hydraulic toolkit for use in support of outage optimization, management and risk assessment has been developed. This mechanistic toolkit incorporates simple models of key thermal-hydraulic processes which occur during an outage, such as recovery from or mitigation of outage upsets; this includes heat-up of water pools following loss of shutdown cooling, inadvertent drain down of the RCS, boiloff of coolant inventory, heatup of the uncovered core, and reflux cooling.

This paper provides a list of key toolkit elements, briefly describes the technical basis and presents illustrative results for RCS transient behavior during reflux cooling, peak clad temperatures for an uncovered core and RCS response to loss of shutdown cooling.

1.0 INTRODUCTION

EPRI is developing outage risk assessment and management (ORAM) tools¹ to assist utility personnel in performing safety assessments of outage plans, in assessing risk impacts of proposed scheduling changes for outages in progress, and in evaluating risk levels incurred by contingency actions for recovery from or mitigation of outage upsets. Overall, these tools can be used to help ensure that plant safety perspectives are being addressed in concert with efficient conduct of the outage.

In support of EPRI's ORAM program, SAIC is developing a deterministic thermal-hydraulics toolkit for use in quantifying reactor safety margin during outage activities and in predicting plant response to contingency procedures. These and other applications results are intended to provide input to optimization of outage schedules, to generate insights/technical bases for development/assessment of contingency procedures, to augment the basis for outage planning and control, and to support outage risk assessment and risk management.

Toolkit elements are being assembled in a PC-based thermal-hydraulics package, with capability for menu-driven input parameters and graphical display of output results. Formulated models and results generation algorithms are designed to provide applications information in much less than real time. The toolkit application results can be used to enhance: (i) outage optimization information (such as system response time constants for use by outage planners in shortening outage time, reducing manpower requirements, and establishing the best way to achieve an outage objective), (ii) contingency procedures technical basis (including time available for diagnosis of and recovery from an outage upset, rates/integral requirements for achieving a success criterion, and input to development of procedures for protecting/ensuring a safety function), and

(iii) outage planning alternatives (such as feasibility/effectiveness of safety/nonsafety-grade systems for use in recovering from an outage upset or realizing a planned objective).

Currently developed elements of the ORAM thermal-hydraulics toolkit are summarized in Table 1. These are grouped in two types: those dealing with plant response (Type I) as well as others of a database nature (Type II). Also included in the table are plant configuration options for each toolkit element as appropriate for (U.S.) vendor designs. The current emphasis in toolkit development is decay heat removal as related to inventory management and as may be impacted by inadvertent leakage.

Brief descriptions of toolkit models and/or methods of solution are given in the next section. This is followed by discussion of illustrative results for representative case studies including reflux cooling (#6), peak clad temperature (#8), and RCS response to loss of shutdown cooling (#9). The paper then closes with a brief summary of ongoing and proposed future work.

2.0 TOOLKIT MODELS

Since a given physical model (such as heatup of a water pool) may be present in more than one toolkit element, this section addresses the distinct models utilized. For brevity, attention is given to key features of the technical basis.

2.1 Heatup of Water Pools

Heatup of water pools via decay heat generation is simulated by means of simple thermal mixing models. When water level is higher than the tops of fuel bundles, a two-mass natural circulation model is applied wherein thermal equilibrium between water and immersed structure is assumed for both fuel-bearing and above-fuel regions. Loop natural circulation rates are extracted from a balance between buoyant head (proportional to the density difference of "hot"/"cold" water zones) and the hydraulic resistance of presumed equi-area pathways for upwards/downwards flow. Both form and friction drag are considered; when flow branching is present (e.g., the upper vessel in parallel with hot leg/pressurizer/steam generator portions of a PWR), network theory is applied to extract an effective loss coefficient.

When water level is below the upper bundle ends, a single well-mixed control volume is utilized with (of course) decay heat generation being partitioned between covered and uncovered portions of the fuel. (As described below, the assumption of perfect mixing in a given region extends to cases in which inflow of injected water is present.)

2.2 Convective Cooling of Immersed Fuel

For cases in which throughput of injected water results in partial, or complete, decay heat removal (e.g., via gravity drain cooling), the exiting flow is assumed to be in thermal equilibrium with resident fuel/water (100% effective heat exchanger). Although this approach is not "conservative," hand calculations show that the resultant overprediction of cooling rates is not consequential.

2.3 Leak/Drain Rates

For loss of coolant inventory via leaks or scheduled openings in the coolant pressure boundary, simple hydraulic network theory is applied, assuming that inertial forces are negligible. Since the RCS may be closed and partially pressurized, the driving force for flow is taken to be the sum of the liquid-side barometric head and overall pressure difference. In general, the flow resistance head is the integral contribution of form/friction losses.

For the special case of gravity drain cooling via the RWST, variable throttling of the drainage flow, subject to core exit temperature levels being less than saturation, is simulated; this is done to reflect the likelihood that operators will optimize coolant utilization. Additionally, flow splits, as incurred by a leakage pathway, are included; this may be due either to an inadvertent leak or from a scheduled opening of the RCS pressure boundary.

2.4 Boiloff of Coolant Inventory

Under saturation conditions, boiloff of coolant inventory occurs. The boiloff rate is equal to the net heat addition rate divided by the latent heat of vaporization, where net heat rate is the difference between decay power generation and heat removal rates owing to convective cooling and/or heat transfer to colder surroundings. (For RCS configurations which are closed, pressurization of the RCS gas space occurs, with attendant increases in saturation temperature levels; the associated effects of sensible energy storage and reduced latent heat magnitudes are also included in the modeling.)

2.5 Peak Clad Temperature

For circumstances in which makeup is insufficient to balance boiloff from a fully covered core, the upper portion of the core is uncovered. For such a case, clad temperatures maximize at values for which convective cooling by boiloff steam from the covered portion of the core is sufficient to balance decay heat generation. A complication is the spatial variability in decay power peaking factors, which may result in temperature peaking below the top of the core.

Employing a discrete approach, the uncovered portion of the core is subdivided into an axial sequence of control volumes. Starting at the lowermost control volume next to the water surface, steady state heat balances are sequentially applied in which nodal decay power is removed via convective heat transfer, the incoming steam temperature being that exiting from the control volume below. The temperature difference between clad and flowing steam is equal to the ratio of decay power per unit elevation divided by the product of heat transfer coefficient and wetted perimeter. Required transfer coefficients are calculated via standard correlations for laminar, transition, and turbulent flow.² The effects of power peaking factors are incorporated via input from toolkit element #14.

2.6 Single Bundle Heatup in Air

In the event that water cooling is lost during fuel transfer to the spent fuel pool, bundle heatup in air may occur. Assuming

unidirectional flow of free convection air, bundle heatup is analyzed as described above for peak clad temperature. Here, however, the inlet temperature to the lowermost "node" is that of ambient air. (For PWR bundles, this approach may be overly conservative since transverse flow of entrained air is expected along the bundle axis; this provides more effective heat removal and lower peak temperatures.)

2.7 Reflux Cooling

Following loss of RHR, a contingency strategy for decay heat removal is use of the steam generators in the reflux cooling mode. This can be effective if the RCS is intact such that pressure can increase, resulting in flow of steam-air mixture through the hot legs and into the steam generator tubes. The steam component of the mixture then condenses along the entry portion of the tube walls, air in the system being gradually displaced into the downstream ends of the tubes. For U-tube designs, condensate drains back into the core via the hot legs and upper plenum; while, for once-through designs, drainage occurs via the cold legs.

The present model for reflux cooling consists of three coupled control volumes:

- (1) The RCS gas volume external to the steam generator tubes, neglecting [any] residual volume on the cold-leg side of the steam generators.
- (2) The RCS gas volume contained within the steam generator tubes and [any] residual gas volume on the cold-leg side.
- (3) The liquid volume on the steam generator secondary sides.

For the first control volume, boiloff steam mixes with resident steam-air mixture, inducing flow of steam and air to the steam generators. The composition of the flowing mixture is specified parametrically via an entrainment "law"; one limit is the cup-mixed composition. (As will be shown below, the air-displacement phase is relatively fast; thus precise treatment of entrainment is not important.)

Within the second control volume, the effects of noncondensable air on film condensation are accounted for by means of high-rate mass transfer theory correcting both heat and mass transfer coefficients for boundary layer suction.³ Owing to non-linearities in driving forces, the condensation zone is subdivided into a sequence of discrete analysis "nodes," where inflow of steam-rich mixture and outflow of air-rich mixture for each node is dictated by steam removal at the wall, which also governs condensate film mechanics.

In the third control volume, primary-to-secondary side heat transfer results in heatup to saturation and initiation of secondary-side boiling. Depending on the magnitude of decay heat removal requirements, pressure drop across the SG relief valves induces a slightly higher than ambient pressure level and associated increase in steady-state temperature level.

For simplicity, ideal gas behavior is assumed throughout. Further, the temperature of accumulated air in the downstream tube ends is taken equal to that on the secondary side and no credit is taken for heat sinking capacity of component walls. Finally, we assume water level remains at or below mid-loop operation. (As discussed below, high water level would minimize the air entrainment time period.)

3.0 RESULTS AND DISCUSSION

Principal capabilities of the currently developed thermal-hydraulics toolkit for ORAM are illustrated here for elements #6 (reflux cooling), #8 (peak clad temperature), and #9 (RCS response to inventory loss/control). These have been selected to illustrate key applications of the ORAM methodology such as contingency planning and outage management. Plant configurational and other physical parameters are provided as appropriate to each application.

3.1 Reflux Cooling

This toolkit member addresses requirements for and effectiveness of reflux cooling including pressure level and active condenser height needed to sustain decay heat removal. For results generation, the reference plants are a 4-loop Westinghouse PWR, with nominal core power Q_o equal to 3238 MWt and a 2-loop B&W PWR, with $Q_o = 2772$ MWt. Reflux cooling is assumed to initiate at $P^o = 14.7$ psia assuming, further, a saturated steam-air mixture in the gas space at temperature $T^o = 140$ °F. For convenience, the initial temperature on the SG secondary-side is taken equal to that on the primary-side ($T_{ss} = T^o = 140$ °F).

For given time t_o from reactor shutdown, the steam generation rate may be approximated by⁴

$$\dot{m}_{stm} (\text{lb}_m/\text{s}) = Q_{dk}/\hat{h}_{fg} = (90 Q_o/t_o^{0.26})/\hat{h}_{fg}$$

where Q_o is in MWt, t_o is in seconds, and \hat{h}_{fg} is latent heat of vaporization (Btu/lb_m).

Requirements for reflux cooling are presented for two time periods. During the first period, sweep-out of air into the downstream end of (active) steam generators occurs. During the second (longer-term) period, sustained heating of secondary-side water to boiling conditions takes place; it is assumed that the heat load is equal to decay heat generation ($90 Q_o/t_o^{0.26}$)

U-Tube Steam Generator Designs

For U-tube (Westinghouse) designs, the reference steam generator contains 4578 Inconel U-tubes of average length $L_T = 57.4$ ft, wetted perimeter $\mathcal{P}_w = 796$ ft, and a flow cross-section $A_f = 11$ ft². Assuming a secondary-side water level sufficient to cover the U-bends, $V_{f,ss} = 1860$ ft³. Taking a mid-loop water level on the primary side, the overall primary-side gas volume is about 5400 ft³ for 4 steam generators active, giving an (initial) air partial volume

$$V_{air}^o = \frac{P^o - P_{sat}(140 \text{ °F})}{P^o} V_{PS} = \frac{14.7 - 2.89}{14.7} 5400 = 4340 \text{ ft}^3$$

For this case, reflux cooling is quickly established (first time period). As illustrated in Figures 1a through 1c, the time required (which is inversely proportional to \dot{m}_{stm} , i.e., directly proportional to $t_o^{0.26}$) varies from ~1 to ~4 minutes as t_o varies from 10 to 1000 hours. On the other hand, the (intermediate) pressure level required to stabilize reflux cooling only depends on the initial air volume and steam generator alignment. For 4 steam generators active,

$$P_{int} \doteq \frac{V_{air}^o}{n_{sg} A_f L_T} P^o = \frac{4340}{4 \times 11 \times 57.4} \times 14.7 \doteq 25 \text{ psia}$$

which is in close agreement with the asymptote in Figure 1a.

The effects of t_o on the evolution of quasi-steady condensation and active condenser height are displayed in Figures 1b and 1c. For the former, initial mass flow rates to the steam generator are air-rich, which impairs condenser performance despite the (initially) larger condenser areas (compare Figures 1b and 1c at short times). Thereafter, approach to the pure steam limit in the balance of the RCS gas volume (and to the interim pressure level given in Figure 1a) minimizes the effects of air on condenser performance, condensation rates becoming just equal to steam generation rates (asymptotic values in Figure 1b).

The ultimate (primary-side) pressure level required to sustain reflux cooling depends on secondary-side response. For $T_{ss} = 140$ °F and assuming heatup to boiling at a relief-valve pressure $P_{ss} = 24$ psia, the time interval involved is given by $\Delta t_{ss} = n_{sg} (\rho_f c_f V_f)_{ss} (T_{sat} - T_{ss}^o)/Q_{dk}$.

Taking $\rho_f = 63$ lb_m/ft³, $c_f = 1.0$ Btu/lb_m-°F, $V_f = 1860$ ft³, $T_{sat} (24 \text{ psia}) = 238$ °F, $Q_o = 3238$ MWt, $t_o = 3.6 \times 10^5$ s (100 hrs), and $T_{ss}^o = 140$ °F, $\Delta t_{ss} = 4390$ s.

During this interval, the primary-side pressure response is a complex function of air-bubble thermal-mechanics including (1) thermal equilibration with the secondary side, (2) humidification of the (drying) air, and (3) pressurization of the "bubble." Since, as shown in Figure 1c, the condenser height is small (and must remain so), the above effects can, to good approximation, be represented by

$$P_{PS} = \frac{T_{ss}}{T_{int}} P_{int} + \eta P_{sat}(T_{ss})$$

where $0 \leq \eta \leq 1$ is efficiency of the humidification process.

Taking, for example, $\eta = 1$

$$P_{PS,max} = \frac{238 + 460}{140 + 460} \times 25 + 24 = 53 \text{ psia}$$

Parametric calculations via the PC-based model are presented in Figure 1d, where small corrections for active condenser volume, based on film condensation of pure steam, are included.

Once-Through Steam Generator Designs

For once-through (B&W) designs, the reference steam generator contains 15,531 tubes of length $L_T = 52$ ft and flow cross-section $A_f = 26.3$ ft². For comparison purposes, we take $V_{PS} = 5400$ ft³ (as for the Westinghouse case) and $V_{f,ss} = 3453$ ft³. Shown in Figure 1d are results for pressure response at $t_o = 10$ hours and $n_{sg} = 2$. Not surprisingly, the results are similar to those for Westinghouse (note the $n_{sg} = 2$ versus $n_{sg} = 4$ scaling on control volume/surface considerations).

3.2 Peak Clad Temperature

This member of the toolkit calculates steady-state temperature distributions in a partially (or wholly) uncovered core. For results generation, makeup to the core is assumed to just balance boiloff for a specified water level, the temperature of the injection flow being a parameter. The reference plant is a 3238 MWt

PWR; the core design consists of 177 fuel bundles, each bundle containing 15×15 lattice positions. The wetted perimeter, P_f in the uncovered region is about 4470 ft with an axial flow area $A_f = 53.4 \text{ ft}^2$, giving a hydraulic diameter $D_n = 0.048 \text{ ft}$.

For the presumed uni-directional flow of generated steam in the uncovered portion of the core, clad temperature distribution is dominated by the power peaking factor distribution, $P_k(z)$, which is taken here as the mean of beginning and end of life fuel (see Figure 2a); this is illustrated in Figures 2b through 2d. As may be seen, peak clad temperature occurs at positions intermediate between the water level (note dimensionless core heights $z_f^* = 0.5$ and 0.75) and the core exit ($z^* = 1$). This is due to the aforementioned Figure 2a power distribution, the effect being tempered by convective heat transfer to flowing steam wherein maximum thermal driving forces obtain near the extreme in peak clad temperature distribution (see Figure 2b). As required, peak clad temperature increases with decreasing water level (i.e., decreasing steam flow); as water level approaches the core mid-place, values exceed the design-basis and approach levels at which autocatalytic clad oxidation is of concern ($T_{\text{clad}} \rightarrow 2600 \text{ }^\circ\text{F}$ — note the $z_f^* = 0.5$ case in Figure 2b).

The effects of time from reactor shutdown (t_0) on peak clad temperature are illustrated in Figures 2c and 2d taking, respectively, $T_{\text{inj}} = 140 \text{ }^\circ\text{F}$ and $T_{\text{inj}} = T_{\text{sat}} = 212 \text{ }^\circ\text{F}$. As $t_0 \rightarrow \infty$, the aforementioned dominance of axial power distribution is overcome by convective heat transfer, clad temperature tending to track with the gas temperature distribution (compare for example, the $z_f^* = 0.5$ cases in Figures 2b and 2c with, for the latter, $t_0 = 500 \text{ hr}$). This effect is also evident in Figure 2d where injection of saturated water, which maximizes steaming rates, is seen to reduce peak clad temperatures and the associated impact of nonuniform power distribution.

3.3 RCS Response to Loss of SDC and Coolant Leakage

We close the presentation of illustrative results with a situation in which shutdown cooling (SDC) is lost in tandem with loss of coolant inventory via an inadvertent leak. The reference product line is a BWR-6 with $Q_o = 3833 \text{ MWt}$; for completeness, partial makeup (corresponding to typical CRD flows) is assumed at a fixed rate $\dot{V}_{\text{inj}} = 100 \text{ gpm}$. The leak elevation is taken to be the RPV/RHR outlet line (15 ft above the inside bottom of the vessel); in concert with presumed flood-up to the top of the steam dryers ($z_f^* = 52 \text{ ft}$), this gives a maximum 37 foot head difference for driving the (initial) leakage flow. Conservatively, heat sinking credit is taken only for the contiguous core and above core regions giving, respectively, $(\dot{M}c)_{\text{hot}} = 1.09 \times 10^5 \text{ Btu/}^\circ\text{F}$ and $(\dot{M}c)_{\text{cold}} = 1.10 \times 10^5 \text{ Btu/}^\circ\text{F}$, the latter decreasing as inventory levels drop. For simplicity, representative loss coefficients in the leak line and within the RPV thermal mixing zone are taken, respectively, as 10 and 74, the latter also decreasing as inventory levels drop.

Typical results for thermal-hydraulics response to loss of SDC in concert with net leakage of RPV inventory are presented in Figures 3a through 3c. As shown in Figure 3a, the potential for onset of boiling (or entry into "hot" shutdown, i.e., OPCON 3) within the first half hour after loss of SDC is markedly diminished for outage periods exceeding, say, 30 days, despite the fact that water level drops below the top of the core (see Figure 3b). This is due, in part, to the heat sinking capacity of the makeup flow, which is assumed to enter the RPV at the initial water temperature ($T^0 = 140 \text{ }^\circ\text{F}$).

An appreciation for the effectiveness of thermal mixing is illustrated in Figure 3c, where mass flow rates for thermal mixing, inventory leakage, and steam generation are compared for the $t_0 = 10 \text{ hr}$ case. (Thermal mixing is, of course, terminated when water level drops below the top of the core.) (As may be surmised, the temperature offset between the core and above core regions is predicted to be small, on the order of $1 \text{ }^\circ\text{F}$; thus, a homogeneous lumped capacitance model would appear justified.) The estimated leakage rates ($\dot{m} \approx 180 - 100 \text{ lb/s}$, or about $1300 - 720 \text{ gpm}$) are similar in magnitude to other estimates for drain down via the RHR drain path.⁵

4.0 CONCLUDING REMARKS

Capabilities of a thermal-hydraulic toolkit for use in outage risk assessment and management have been described. For representative members of the toolkit, PC-based solutions of the governing equations have been presented with emphasis on parameter variation of interest to outage planning and control. In addition, simplified algebraic expressions, amenable to hand calculations, have been formulated and comparisons for key results provided.

For the case of reflux cooling as an alternative strategy for decay heat removal, two distinctive time periods for stabilization of the process are addressed. For the first (brief) period, noncondensable air is swept to the downstream ends of steam generator tubes; at the end of this period (1-4 minutes), transition to condensation of pure steam is applied. Thereafter, gradual heatup of secondary-side water occurs in tandem with partial humidification of accumulated air; depending on the extent of humidification, this period may control the magnitude of RCS pressure rise.

In the event that partial uncovering of the core occurs, peak clad temperatures are shown to be first-order dependent on axial power peaking factors. As water level approaches the core mid-plane, maximum temperatures approach levels ($T_{\text{clad}} \rightarrow 2200 \text{ }^\circ\text{F}$) at which autocatalytic oxidation by steam is a concern. In addition to these (steady-state) results, transient results for heatup of a (bottom-peaked) BWR core have been generated, assuming a fully uncovered core. For times from reactor shutdown equal to 10, 100, and 1000 hours, peak clad temperatures approach oxidation conditions at elapsed times $t = 31.6, 57.5, \text{ and } 104.6$ minutes, respectively. Finally, for an uncovering core, capability (not shown) for tracking water level and thermal response of the uncovered fuel has been included as parts of toolkit element #9.

5.0 REFERENCES

1. S. PAL KALRA, "Managing the Safety of Shutdown Plants," *ATOM*, Vol. 424, pp. 26-28 (1992).
2. D. K. EDWARDS et al., *Transfer Processes: An Introduction to Diffusion, Convection, and Radiation*, Hemisphere/McGraw Hill (1979).
3. W. M. KEYS, et al., *Convective Heat and Mass Transfer*, McGraw-Hill Book Co., New York (1966).
4. "Severe Accident Management Guidance Technical Basis Report," Appendix R, EPRI, TR-101869 (1992).
5. Personal Communication, J. Hewitt, Engineering Research, Inc. (1993).

Table 1. Thermal-Hydraulic Toolkit for ORAM
 – Plant Response Toolkit Elements (Type I) –

#	Tool Kit Element	Plant Configuration
1	Time-to-boil of RCS/ refueling pool inventory	<ul style="list-style-type: none"> • Vessel head on/off • With/without participation of refueling pool • With/without participation of steam generators • With/without heat removal • Head detension leakage and letdown flow • Partial/full in-vessel fuel loadings
2	Time-to-boil of spent fuel pool	<ul style="list-style-type: none"> • Variable fuel loading • With/without heat removal • Makeup/letdown flows • Variable initial inventory
3	Gravity drain cooling via RSWT	<ul style="list-style-type: none"> • Vessel head on/off • RSWT drainage with/without throttling • Multiple leak/spill paths • With/without by-pass of injected flow
4	Gravity-drain cooling via refueling pool	<ul style="list-style-type: none"> • Vessel head off • Multiple leak/spill paths • With/without by-bass of injected flow
5	Inadvertent drainage of RCS/ refueling pool	<ul style="list-style-type: none"> • Vessel head on/off • Multiple leak paths • With/without makeup • With/without heat removal • Partial/full in-vessel fuel loadings
6	Reflux cooling	<ul style="list-style-type: none"> • UTSG, OTSG, and IC RCS pressure levels required to sustain reflux cooling • Variable number of participating steam generators • With/without secondary-side makeup • With/without RCS venting
7	Boiloff of RCS inventory	<ul style="list-style-type: none"> • Vessel head on/off • With/without makeup, letdown and leaks • With/without heat removal • In-vessel/in-core level tracking
8	Peak clad temperature	<ul style="list-style-type: none"> • Transient heat up of uncovering core • Steady-state limit for clad temperatures • Makeup required to maintain in-core temperature/water levels
9	RCS response to inventory/pressure control	<ul style="list-style-type: none"> • Vessel head on/off • With/without makeup, letdown • Participation of valves, manways and leak paths • With/without gas phase vent paths
10	Flow rates for RCS vent paths	<ul style="list-style-type: none"> • Gas/liquid vent/leak rates • Required flows for RCS pressure control • Containment mass/energy loadings
11	Inadvertent drainage of spent fuel pool	<ul style="list-style-type: none"> • With/without heat removal • With/without makeup
12	Single bundle heat up	<ul style="list-style-type: none"> • Transient heat-up of single bundle hanging in air • With/without air cooling

Plant Data Base Toolkit Elements (Type II)

13	RCS thermal-hydraulic parameters	<ul style="list-style-type: none"> • Area/volume vs. elevation • Representative flow resistances • Representative heat structure thermal masses
14	Decay power and stored energy	<ul style="list-style-type: none"> • Decay power generation rates • Stored thermal energy inventories

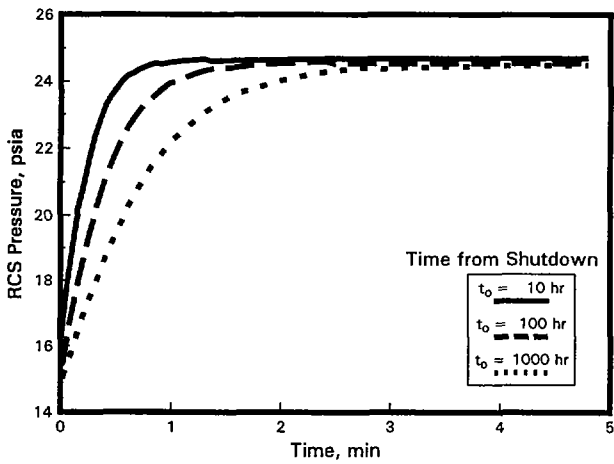


Figure 1a - RCS Pressure Response to Establishment of Reflux Cooling ($n_{sg} = 4$).

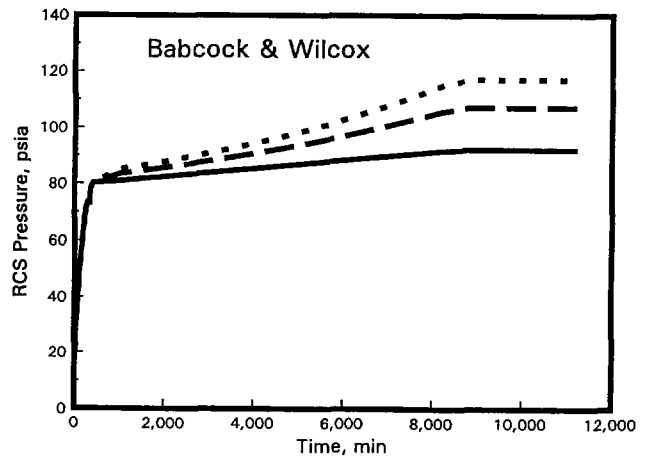
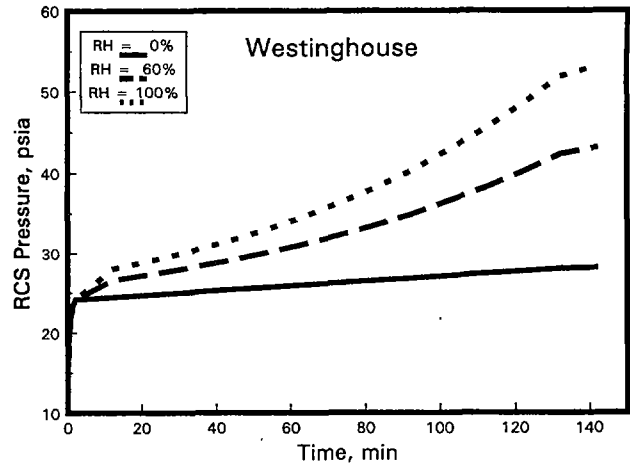


Figure 1d - Effects of Humidification Extent for Accumulated Air on RCS Pressure Response to Reflux Cooling.

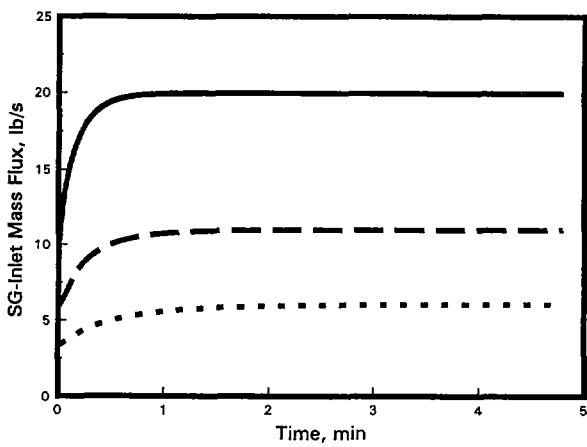


Figure 1b - SG Inlet Mass Flow Rates During Establishment of Reflux Cooling ($n_{sg} = 4$).

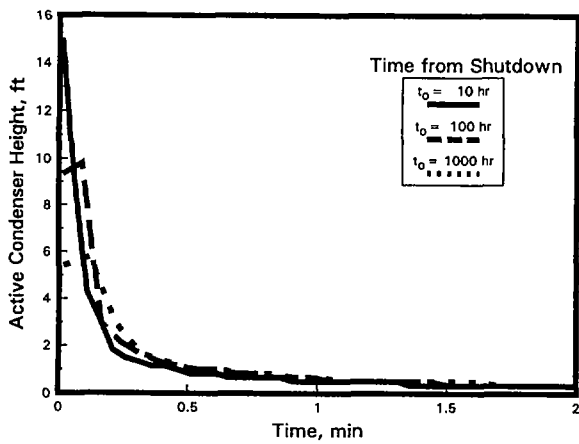


Figure 1c - Active Condenser Height During Establishment of Reflux Cooling ($n_{sg} = 4$).

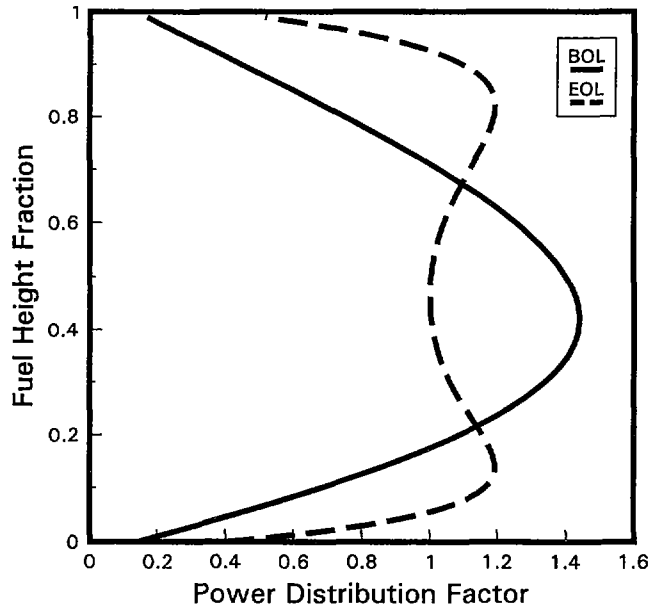


Figure 2a - Axial Power Distributions for Beginning and End of Life.

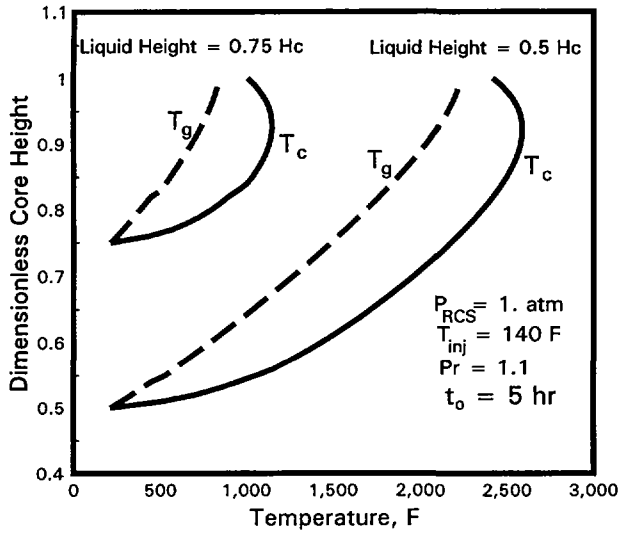


Figure 2b - Axial Temperature Distributions for Clad (T_c) and Flowing Steam (T_g) in the Uncovered Core.

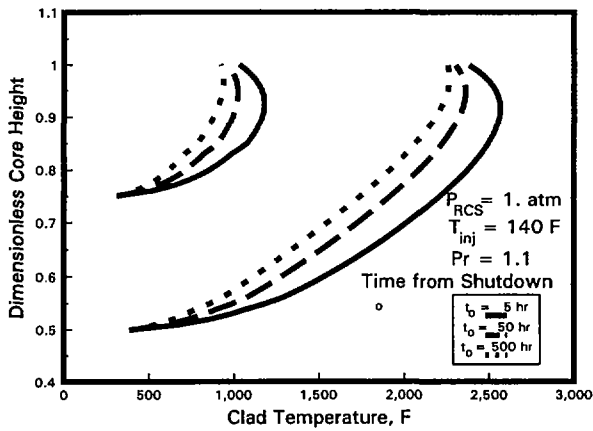


Figure 2c - Clad Temperature Distribution in the Uncovered Core as a Function of Collapsed Liquid Height and Time From Reactor Shutdown ($T_{inj} = 140 \text{ }^\circ\text{F}$).

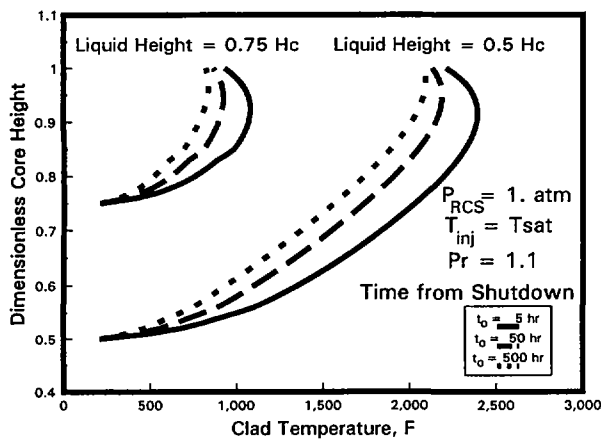


Figure 2d - Clad Temperature Distribution in the Uncovered Core as a Function of Collapsed Liquid Height and Time From Reactor Shutdown ($T_{inj} = T_{sat}$).

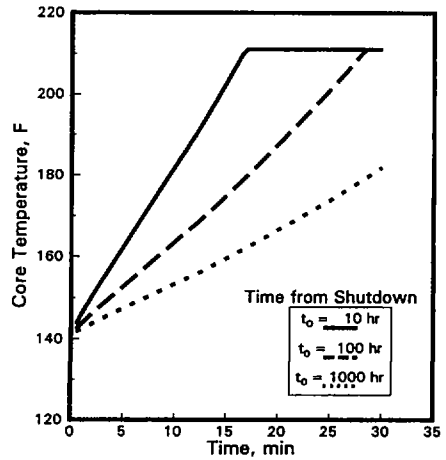


Figure 3a - Temperature Response of BWR Water Inventory to Loss of RHR, Inadvertent Leakage, and Partial Injection ($\dot{V}_{inj} = 100 \text{ gpm}$).

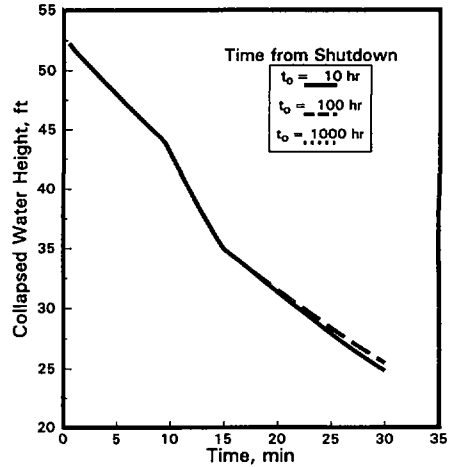


Figure 3b - Response of Collapsed Water Level to Loss of RHR in the Presence of Inadvertent Leakage and Partial Injection ($\dot{V}_{inj} = 100 \text{ gpm}$).

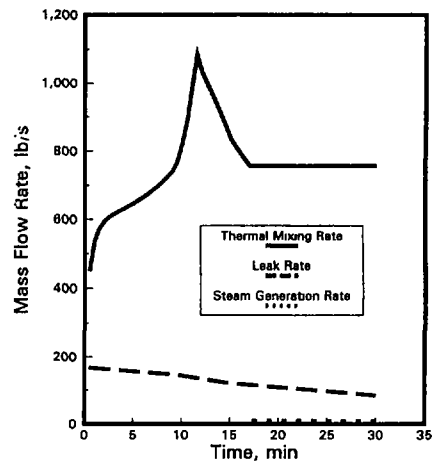


Figure 3c - Mass Flow Rates Following Loss of RHR in the Presence of Inadvertent Leakage and Partial Injection ($\dot{V}_{inj} = 100 \text{ gpm}$).